Chapter 14

Data Mining from Remote Sensing Snow and Vegetation Product

Gao Jie

Additional information is available at the end of the chapter

http://dx.doi.org/10.5772/45732

1. Introduction

Snow is an important research interest in international cryosphere research. In China, cold region account for 43% of the total area (Yang et al., 2000). The area of stable snow where snow cover duration is greater than 60 days is approximately $420 \times 10^4 km^2$. In West China, the recharge to spring freshet from winter snow is a necessary regulation for spring drought (Qin et al., 2006). However, larger area but sparser stations in West China lead to a shortage of observations. Especially for snow, most of the regions where snow-dominated are located in mountainous regions that are quite inconvenient for people to establish observatory stations. All these result in a poor representative of station observations (Li, 1995). Therefore, application of Remote Sensing is absolutely necessary for snow research (Gao et al., 2010).

The data received and released by the Moderate-resolution Imaging Spectroradiometer (MODIS) with a spatial resolution of 250m, 500m and 1000m have been widely used for research. Huang et al (2007) combined Geographic Information System (GIS) and station observations to analyze the precision of snow identification of two types of MODIS snow products: MOD10A1 (daily snow cover data) and MOD10A2 (8-day snow cover data) in Northern Xinjiang area. 8-day data is proved to better eliminate the influence of amount of clouds and with a mean precision of snow identification about 87.5%. Wen et al (2006) assessed the seasonal variation of snow extent in parts of Nyainqntanglha Range (4720-5850m) based on MODIS data, and proved it feasible to monitor snow extent by MODIS data in this region. Zhang et al (2005) revealed that snow-cover area and snow line altitude change obviously with climate change in Qilian Mountains by adopting NOAA-AVHRR, EOS-MODIS data and station observation between May and August, 1997-2004. Han et al (2007) analyzed the feedback of regional snow-cover to climate in Northeast China during 2000-2005 by MODIS products.

Snowmelt hydrological model focus on snowmelt runoff processes and used to quantify snow-related variables in snow water equivalent (SWE). Anderton et al. (2002) developed a grid-based distributed energy balance snowmelt model and used distributed SWE as initial boundary condition. Bell and Moore (1999) developed an elevation-dependent snowmelt forecasting model, and used PACK snowmelt module, which conceptualizes snow storage to 'dry' and 'wet' snow reservoirs with different outflow rates. These methods provide a simple but quantitative relation between snow and water. However, both distributed SWE and reservoir calculate snow as water amount rather than its real state, hardly simulate the spatial pattern of snow covered area, and how it evolves with time. In fact, spatial distribution of snow is very important for hydrological cycle in snowmelt-dominated regions. Whether soil is covered by snow or not is a necessary boundary input for hydrological modelling. It determines the energy balance by albedo, inform whether rainfall runoff generation or snowmelt runoff.

Different factors dominate snow distribution at different scales. At macro-scales (10km–1000km), latitude, elevation, and water bodies primarily control spatial variation of snow. Terrain characteristics and vegetation cover determine at meso-scales (100m–10km), interception, sublimation, and wind redistribution dominate at micro-scales (10m–100 m) (McKay & Gray, 1981; Pomeroy et al., 2002; Liston, 2004). Based on the results of experiments, topographic factors (Marchand & Killingtveit, 2005) and vegetation cover (Jost et al., 2007) are considered to be the most important variables to explain snow pattern at the watershed-scale.

Among all the topographic factors, elevation provides a significant positive correlation with the spatial pattern of snow (Daugharty & Dickinson, 1982; D' Eon, 2004; Varhola et al., 2010) because orographic cooling influence the accumulation and ablation processes of snow (Hendrick et al., 1971; Sloan et al., 2004). Linear lapse rate is regularly observed in mid-latitude mountainous regions (Hantel et al., 2000). Most often, the global mean lapse rate of approximately 6.5°/1000m is common used (Barry, 1992; Li & Williams, 2008). Bell and Moore (1999) adopted 5.9°/1000m in upland British. Based on a statistics of 27-year time series in 7 stations, temperature lapse rate in Eastern Tibet is 6.3°C per 1000 meters, a little smaller than that of 7.0°C per 1000m reported for Colorado Rocky Mountains (Williams et al., 2011; Gao et al., 2012).

Vegetation offers a negative indicator of snow distribution. Calculated from a physically based formulation, interception is closely related to vegetation cover (Hedstrom and Pomeroy, 1998; Pomeroy, 2002). Interception by canopies and increased sublimation reduce snow accumulation on the ground (Essery et al., 2003). In forested area, the amount of snow is 40% lower than in nearby clear-cut reference sites (Winker et al., 2005). Presence of snow affects both length of growing season, and primary plant production (Buus-Hinkler et al., 2006). Long snow-covered periods will shorten vegetative season, for snow-cover prevents the initiation of growing season until it disappears from vegetated areas (Palacios, 1997; Buus-Hinkler et al., 2006). Normalized Difference Vegetation Index (NDVI), an index of vegetation greenness derived from remote sensing data (Jia et al., 2004) is frequently employed. NDVI-related researches in cold regions are frequently conducted. Ones reveal the inter-annual (Myneni et al., 1997; Hope et al., 2003) and intra-seasonal variability of NDVI. Different latitudes (Hope et al., 2004) and vegetation types (Jia et al., 2004) are also assessed. Buus-Hinkler et al. (2006) monitored Snow-NDVI relations at Zackenberg in high Arctic Northeast Greenland at both high spatial and high temporal resolution, and developed a semi-empirical model to calculate snow-cover extent and NDVI. They contributed to establish a detailed relation between vegetation and snow in High Arctic areas. However, less work has been done to relate the spatial patterns of snow cover and NDVI together, and to the altitude in Alpine areas.

In our study, remote sensing data play a critical role in our data mining. Elevation as a variable is considered in spatial distribution of snow, vegetation will be used as a reference, or an indicator. We investigate: (1) quantification of SCA (Snow-Cover Area per unit area of elevation band) – Elevation relations and NDVI-Elevation relations; (2) comparisons among Snow-Elevation-Vegetation relations, to obtain a better understanding of snow-covered area vary with elevation, and the relation to vegetation.

2. Study area and data source

Yangbajain Basin locates at 90°00′E–90°45′E, 29°30′N–30°30′N, southwest of Lhasa River Basin, Tibet China, and southeast of Nyainqntanglha Range. It covers an area of 2665 km^2 and elevation ranges from 3855 to 6970 m (Fig. 2). Permanent snow and glacier develop in this area because of the high altitude and cold weather. Alpine meadow, shrub, and rock cover this mountainous, continental, mid-latitude region.

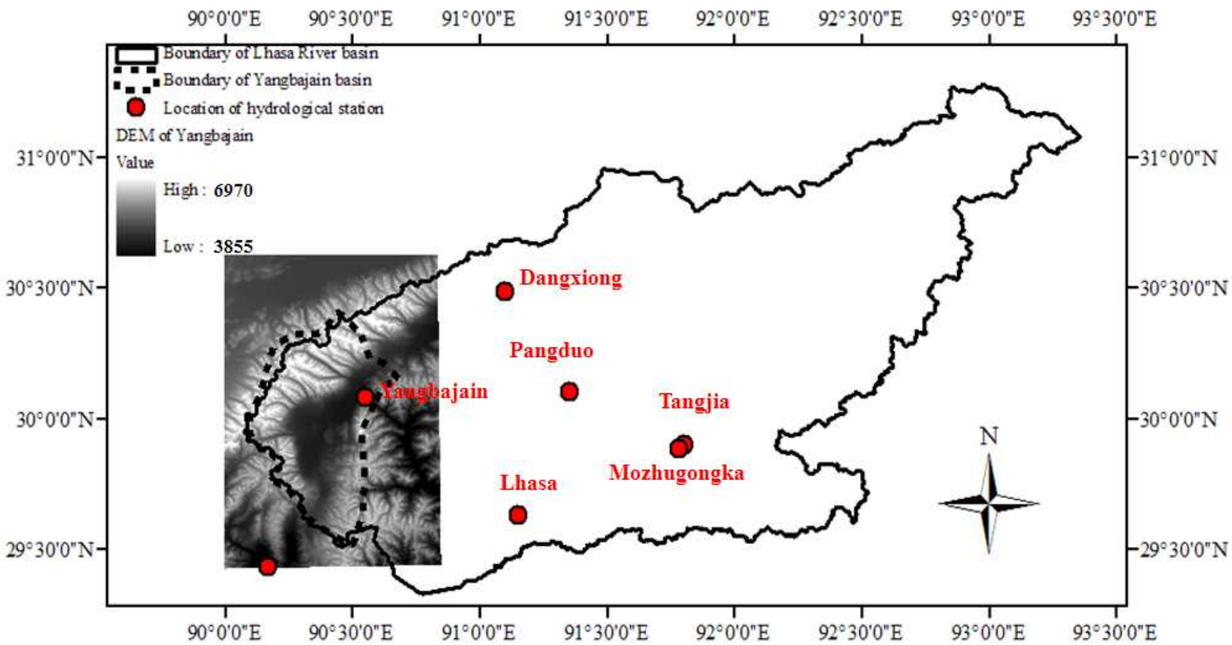

Figure 1. An overview of the study area

Yangbajain Hydrological Station (90°33′E, 30°5′N) is located at the outlet of Yangbajain Basin with an elevation of 4250 m. According to temperature records of the station from

2003 to 2008, annual precipitation in the area averages 505.2 mm, 87.4% of which falls in the summer season from June to September. Monthly air temperature from June to August is above 10°C, with five months: January, February, March, November, and December, having temperatures below 0°C. Monthly average temperature at different elevation bands based on observations at Yangbajain station and interpolated with lapse rate of 6.3°C/1000m are shown in Table 1, elevation bands with air temperature above 0°C are marked in orange, which might indicate an intensive vegetative growth.

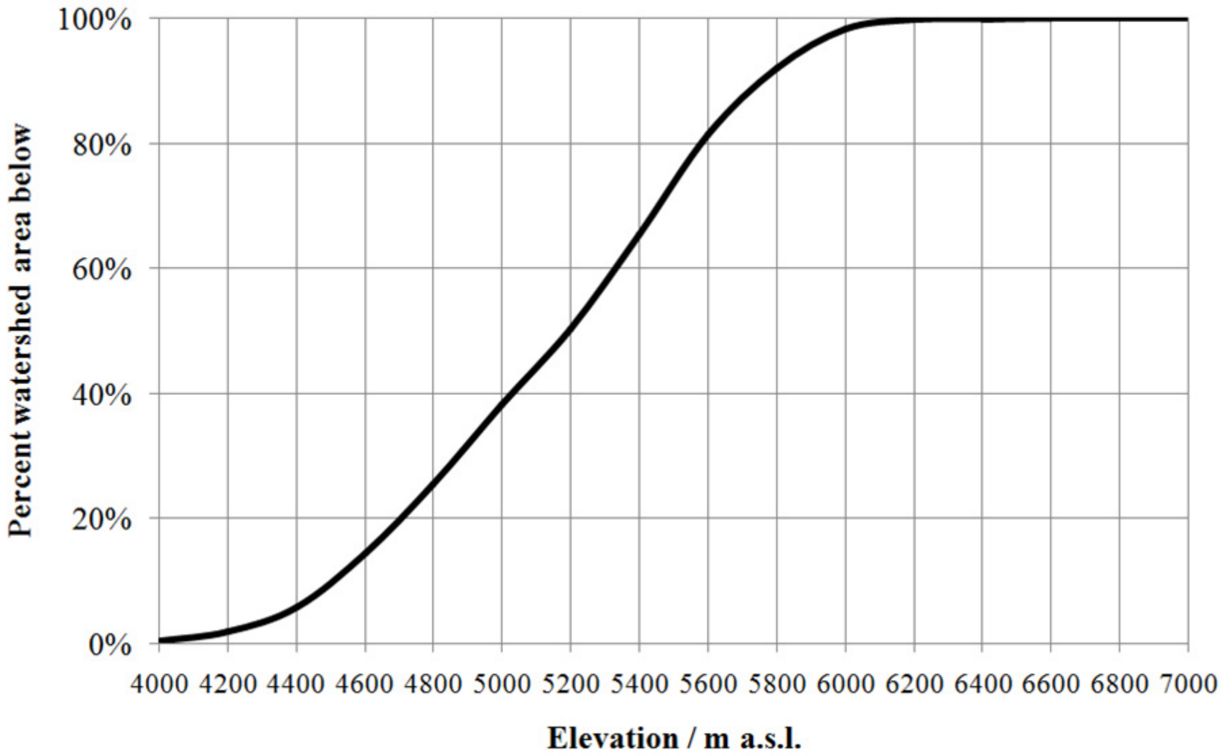

Figure 2. Area-elevation curve for Yangbajain Basin

To examine the relation between SCA and elevation (SCA-Elevation) and Vegetation-Elevation relation, three types of dataset are required:

1. MODIS snow product: MYD10A2 (MODIS/Aqua Snow Cover 8-Day L3 Global 500 m SIN Grid V005) with a resolution of 500 m.
2. MODIS vegetation product: MYD13A1 dataset (MODIS/Aqua Vegetation Indices L3 Global 500 m SIN Grid V005) with a spatial resolution of 500 m and a temporal resolution of 16 days.

Digital Elevation Data (DEM) released by Shuttle Radar Topography Miss (SRTM) version 2 with a resolution of about 90 m.Table 1. Monthly average temperature at different elevation band based on observations at Yangbajain station and interpolated with lapse rate of 6.3°C/1000m.

H (m)	4000	4200	4400	4600	4800	5000	5200	5400	5600	5800	6000	6200	6400	6600	6800	7000
Month	Monthly average temperature (°C) at different elevation band based on observation and lapse rate 6.3°C/1000m															
Jan	-3.2	-4.5	-5.7	-7.0	-8.2	-9.5	-10.8	-12.0	-13.3	-14.5	-15.8	-17.1	-18.3	-19.6	-20.8	-22.1
Feb	-2.3	-3.6	-4.8	-6.1	-7.3	-8.6	-9.9	-11.1	-12.4	-13.6	-14.9	-16.2	-17.4	-18.7	-19.9	-21.2
Mar	1.8	0.5	-0.7	-2.0	-3.2	-4.5	-5.8	-7.0	-8.3	-9.5	-10.8	-12.1	-13.3	-14.6	-15.8	-17.1
Apr	5.0	3.7	2.5	1.2	0.0	-1.3	-2.6	-3.8	-5.1	-6.3	-7.6	-8.9	-10.1	-11.4	-12.6	-13.9
May	9.5	8.2	7.0	5.7	4.5	3.2	1.9	0.7	-0.6	-1.8	-3.1	-4.4	-5.6	-6.9	-8.1	-9.4
Jun	13.0	11.7	10.5	9.2	7.9	6.7	5.4	4.2	2.9	1.6	0.4	-0.9	-2.1	-3.4	-4.7	-5.9
Jul	13.7	12.5	11.2	9.9	8.7	7.4	6.2	4.9	3.6	2.4	1.1	-0.1	-1.4	-2.7	-3.9	-5.2
Aug	13.4	12.1	10.9	9.6	8.4	7.1	5.8	4.6	3.3	2.1	0.8	-0.5	-1.7	-3.0	-4.2	-5.5
Sep	11.4	10.1	8.9	7.6	6.3	5.1	3.8	2.6	1.3	0.0	-1.2	-2.5	-3.7	-5.0	-6.3	-7.5
Oct	6.2	4.9	3.7	2.4	1.2	-0.1	-1.4	-2.6	-3.9	-5.1	-6.4	-7.7	-8.9	-10.2	-11.4	-12.7
Nov	0.1	-1.2	-2.4	-3.7	-5.0	-6.2	-7.5	-8.7	-10.0	-11.3	-12.5	-13.8	-15.0	-16.3	-17.6	-18.8
Dec	-2.6	-3.9	-5.1	-6.4	-7.6	-8.9	-10.2	-11.4	-12.7	-13.9	-15.2	-16.5	-17.7	-19.0	-20.2	-21.5

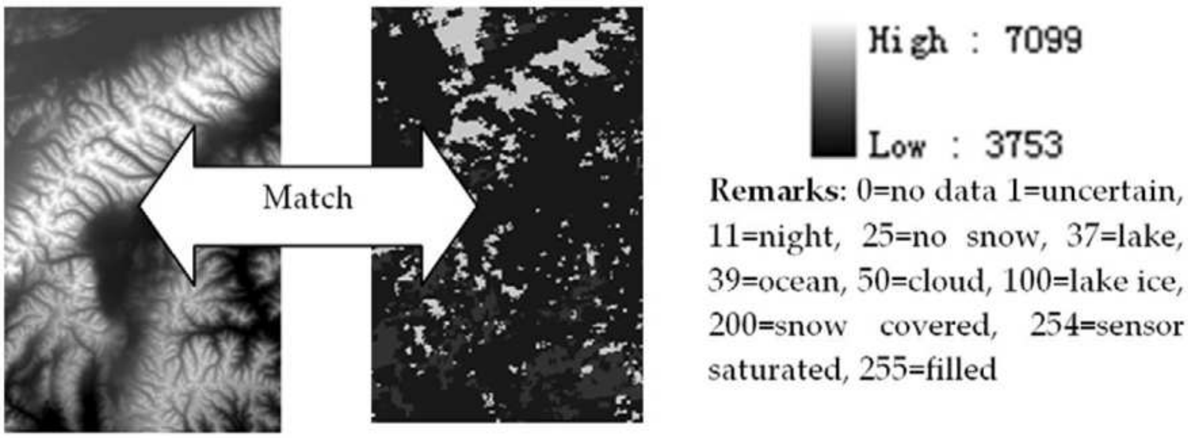

Figure 3. *An example of DEM(left) data and MODIS(right) in gif format*All these datasets are available from https://wist.echo.nasa.gov/. The hdf files of snow product from July 2002 to January 2009, and vegetation product from 2003 to 2005 are adopted in this chapter, except for January 2004 which was unavailable.

The study area involves h25v05 and h25v06 blocks, 226 rows, 150 columns, 33900 grids. The original data are on a Sinusoidal projection. MODIS Reprojection Tools (MRT) provided by NASA is applied for re-projection, mosaic, and extraction. The command: hdftool and hdfread in Matlab is useful for processing the data in hdf format. Programs on C++ language are made to match the DEM and MODIS data (Fig. 3), calculating the average elevation of all the DEM pixels within one MODIS grid. As the spatial resolution of DEM is about 90m, and that of MODIS product is approximately 500m, every MODIS grid has 30 DEM pixels. Thus, we know the elevation for each grid in 6-year MODIS snow products with a time interval of 8-day and 3-year MODIS NDVI products with time interval of 16 days.

MODIS snow grids blurred by cloud are removed under the assumption that average snow cover percentage of cloud-affected grids is similar to average level of the ones without clouds. Finally, every grid in that 6-year/3-year time series contains three types of property: with/without snow, NDVI, and elevation.

3. Temporal distribution of snow and vegetation coverage

Intra-seasonal snow cycle in different elevation zone

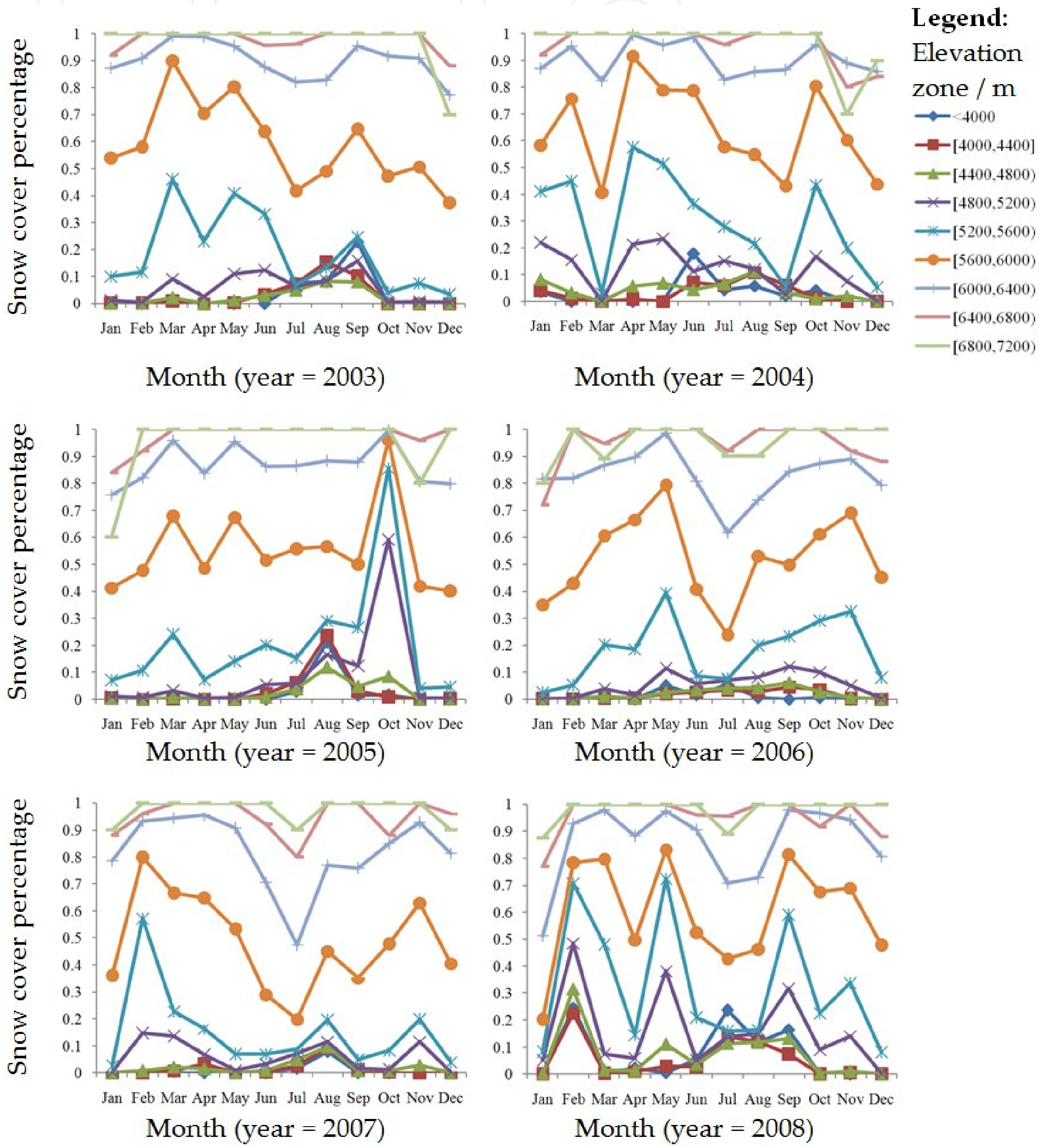

Figure 4. Snow covered and depletion curve in different elevation band from 2003 to 2008

The regions below 4800 m have lower snow coverage, less than 20%. The region above 6400 m is covered by glaciers and permanent snow with snow coverage of more than 70%. In the elevation band between 5600 and 6400 m, the SCA varies but remains 20% at minimum. This is sometimes influenced by the temperature in warm seasons. Seasonal snow covers elevation band between 4800 and 5600 m, and is largely affected by precipitation in winter. The lack of precipitation may lead to snow-free.

Intra-seasonal NDVI variation in different elevation zone

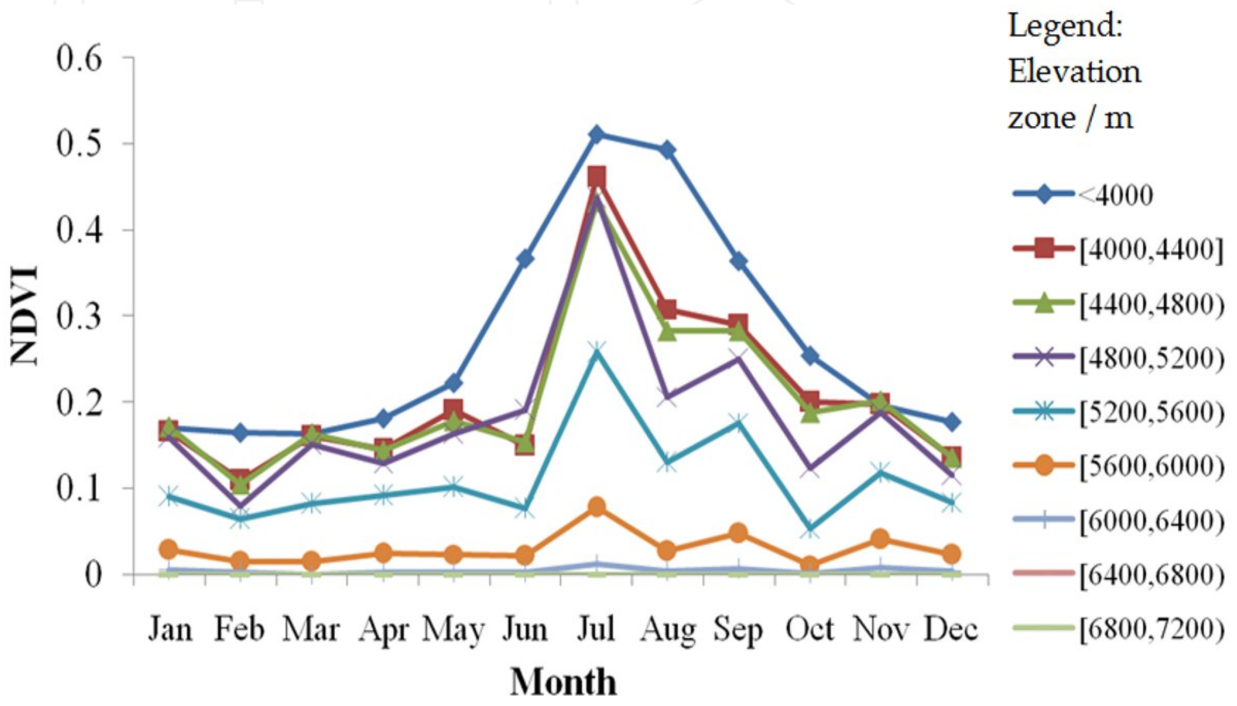

Figure 5. Monthly mean NDVI in different elevation band

A significant seasonality of vegetation is detected in elevations below 5200 m. NDVI values gradually increase from June to July when peak NDVI (>0.3) happens and then decreases. For high elevations (>6000 m), NDVI values remain less than 0.01 during the whole year.

Precipitation and temperature analysis

Precipitation and temperature are considered to be the primary factors which influence snow distribution (Hope et al., 2003), especially winter precipitation and summer temperature. Based on monthly meteorological records from 2003 to 2008, air temperature stays above 0°C from April to October. Figure 6 depicts the monthly temperature anomaly from April to October which indicates melting temperature, while Figure 7 presents the precipitation in January, February, March, November, and December which indicates winter snowfall.

Obvious positive monthly temperature anomalies are recorded in April, August, and October of 2003, May and September of 2004, April and from June to September in 2005, from June to August in 2006, all the warm months except August in 2007 and April of 2008. Furthermore, the decline of SCA occurs within those months, especially in the elevation zone of [5600, 6400] m.a.s.l.

Higher precipitation in February and March of 2007 and 2008 is observed with the total amount of 10.8 and 13.0 mm, respectively. These values are much more than those during the same time of the other four years, which lead to a larger snow-cover percentage at the beginning of those two years. Shortage of snowfall in March 2004 results in the absence of snow below 5600 m.

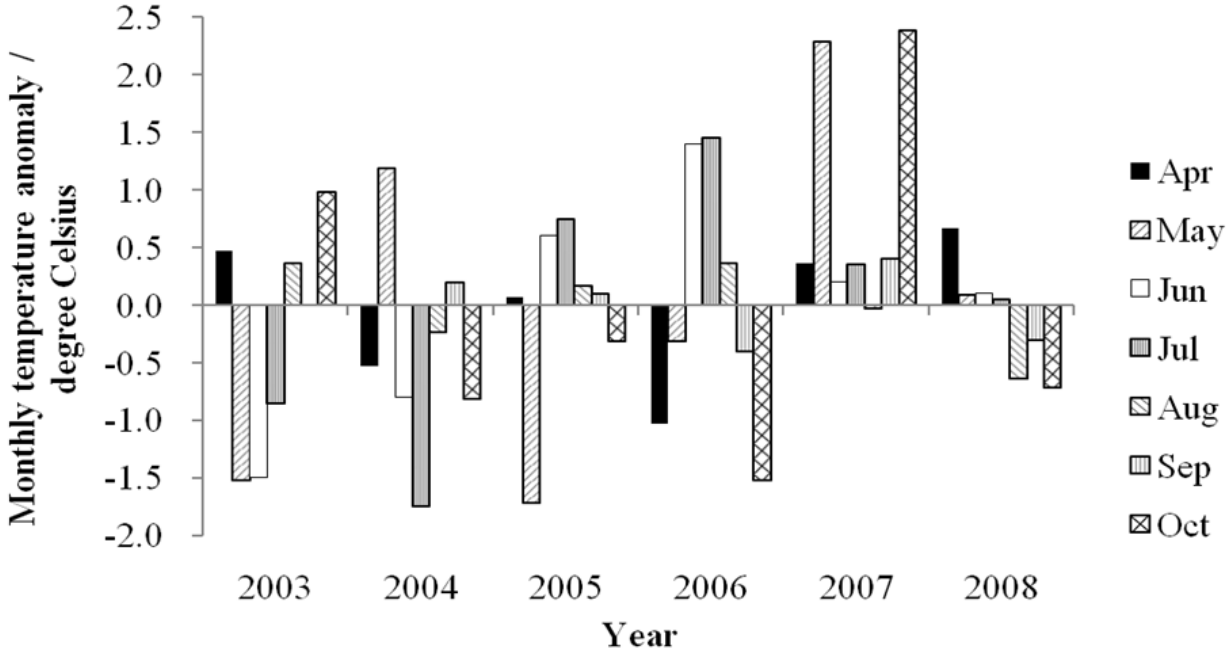

Figure 6. Monthly temperature anomaly from April to Octorber between 2003 and 2008

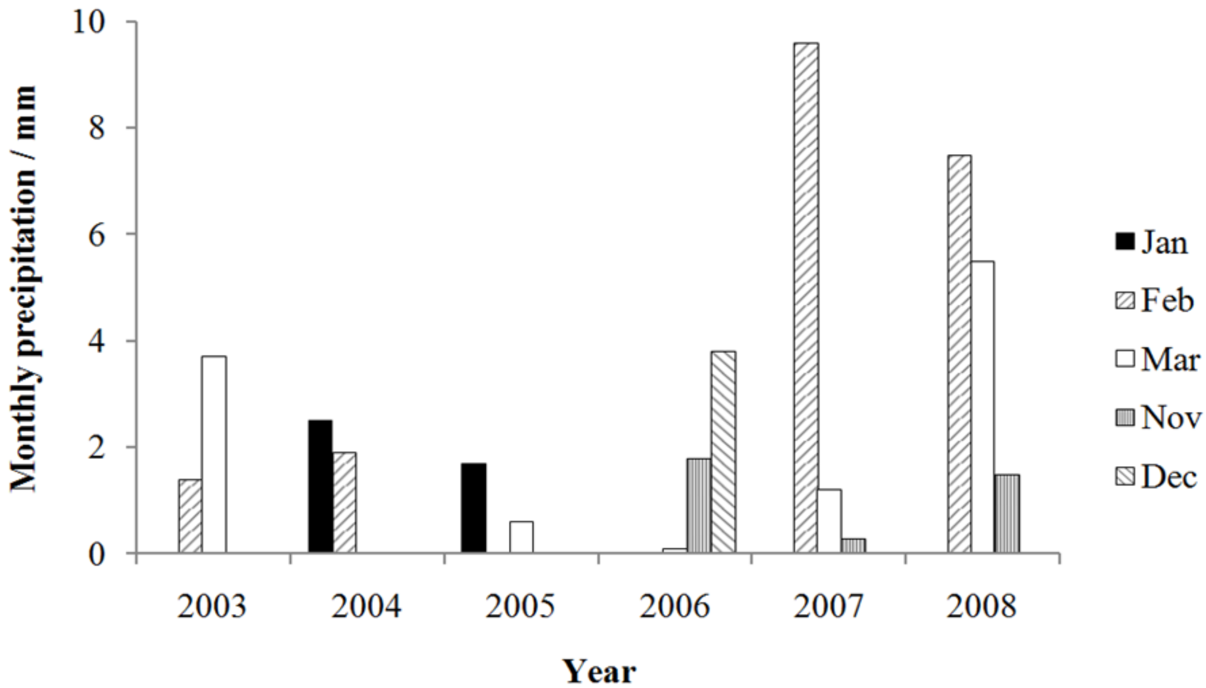

Figure 7. Monthly precipitation from 2003 to 2008 in January, February, March, November, and December

4. Spatial distribution of snow and vegetation coverage

Under a given elevation interval, we sort all the MODIS grids into different elevation band. Therefore, snow cover percentage in one elevation band is counted from the information of with/without snow in the MODIS grids belong to that band. And average NDVI is calculated in that elevation band. In this way, SCA-Month/NDVI-Month relations in different elevation bands are transferred to SCA-Elevation/NDVI-Elevation relations in different months.

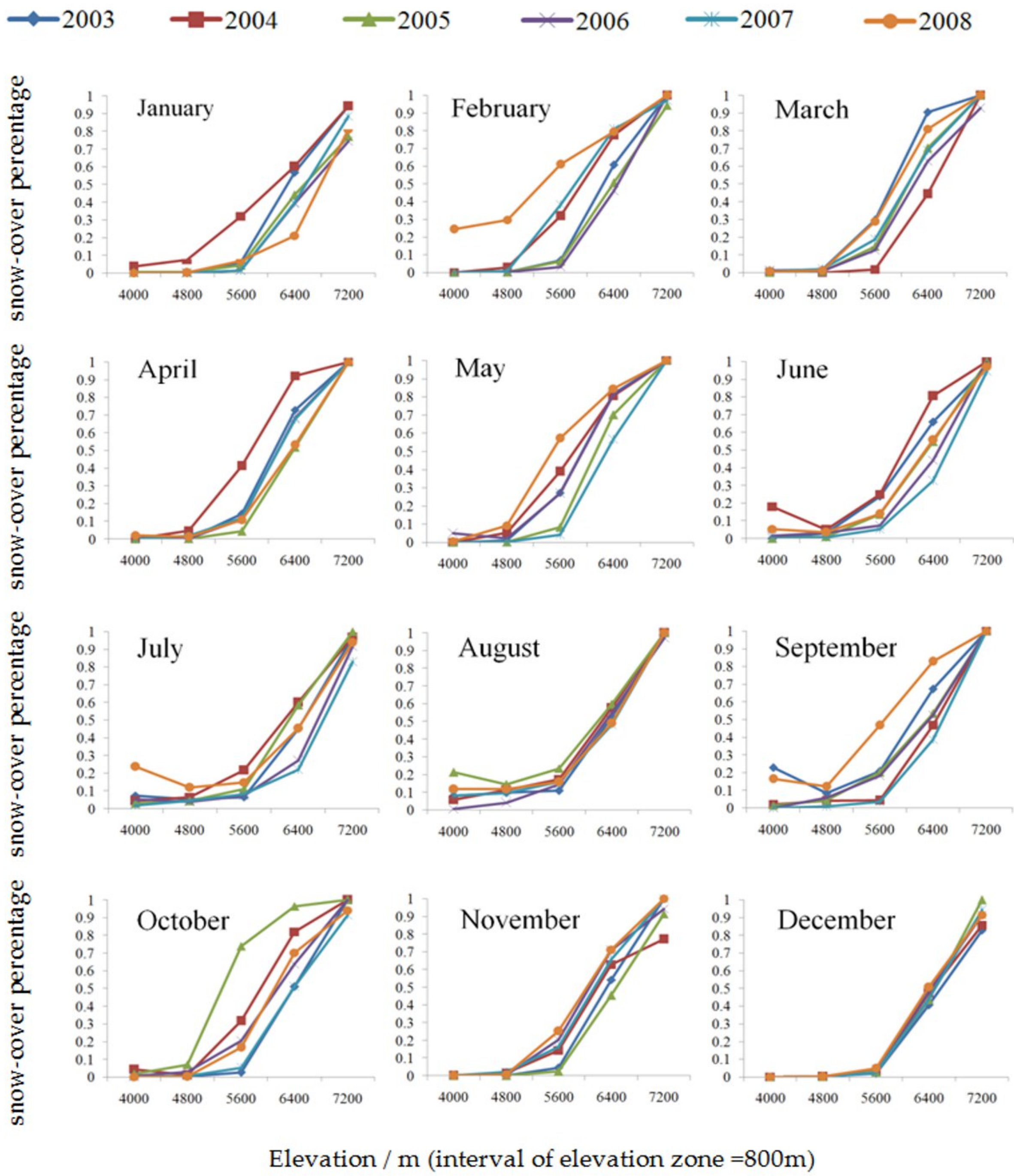

Figure 8. Relation between snow-cover percentage and elevation from January to December during 2003-2008 with an elevation interval of 800 m

Generally, if resolution permitting, the division of a finer elevation interval will help to reveal the results in detail. The resolution of MODIS and DEM are 500 and 90 m, respectively. With a similar magnitude of resolution in both vertical and horizontal directions, the elevation intervals of 800, 400, and 200 m are chosen.

First, we use the elevation intervals 800 and 400 m to discover the relation of SCA-Elevation from 2003 to 2008. Then a comparison between SCA-Elevation and NDVI-Elevation is made based on elevation interval of 200 m from 2003 to 2005.

Two groups are depicted with elevation band intervals equal to 400 and 800 m. In each group, there are 12 figures denoting the 12 months in a year. In each figure, six lines represent the relations of SCA-Elevation in each year from 2003 to 2008 (shown in Fig. 8 and Fig. 9).

The legend is as follows: different shapes denote different years from 2003 to 2008:

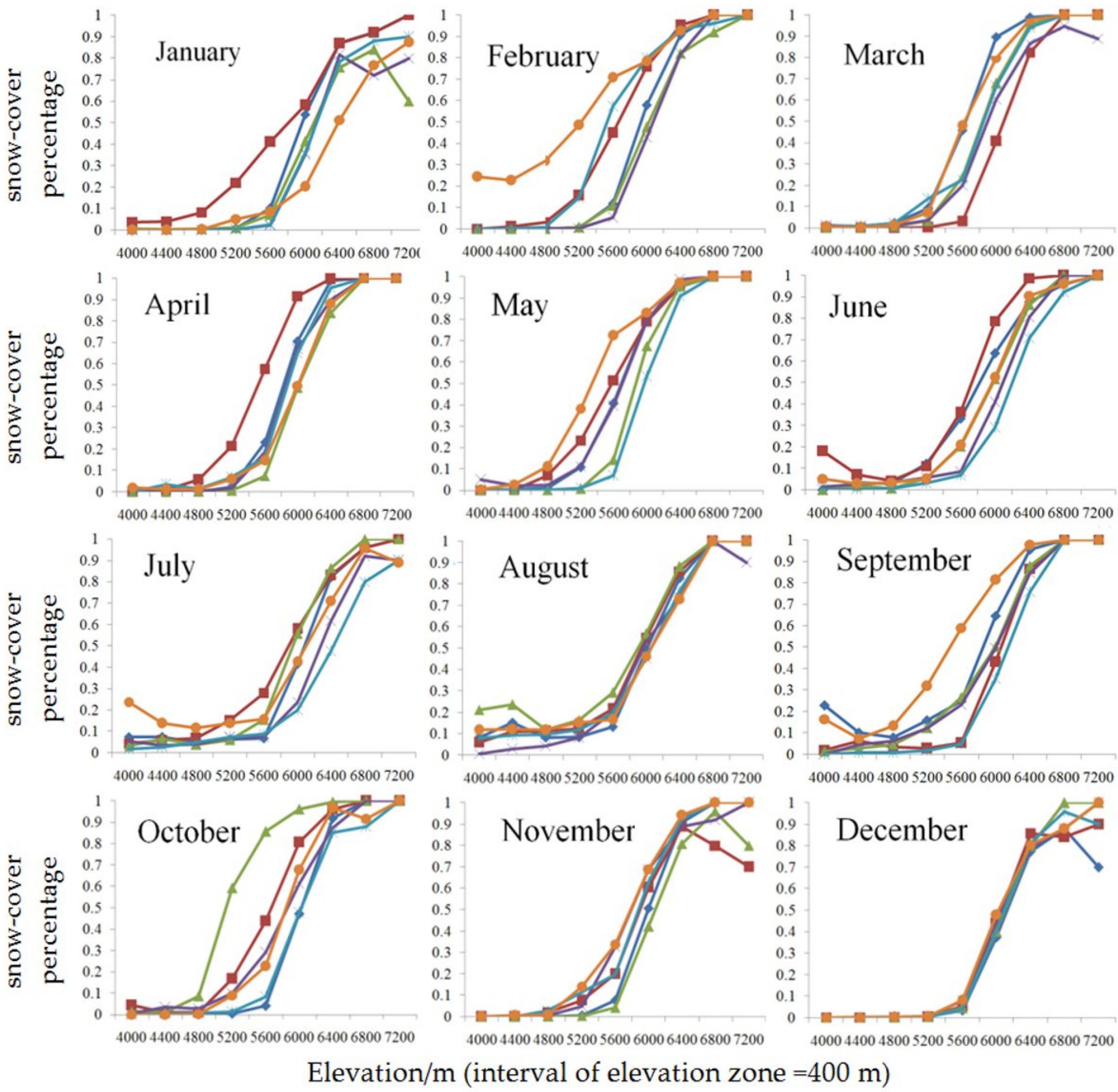

Figure 9. Relation between snow-cover percentage and elevation from January to December during 2003–2008 with an elevation interval of 400 m

The following can be concluded:

1. Based on the division with an elevation interval of 800 m, an obvious positive relation between SCA and elevation is presented. This relation could be considered to be a three-segmented line (Fig. 8) with a slow increase below 5600 m, followed by a rapid rise between 5600 and 6400 m, and finally a lagging growth above 6400 m.
2. If 400 m is used as the elevation interval, the three-segmented line evolves into a smooth "S"-shaped curve in all the months and years (Fig. 9). This is expressed as follows:

$$\frac{dS}{dh} > 0 \tag{1}$$

where S is the ratio of SCA per unit area of elevation zone (Snow-cover percentage).

There exists a critical elevation h_c, which seems to be between 5000 and 6000 m from Fig. 6:

$$\begin{aligned} &if\ h < h_c,\ \frac{dS^2}{d^2h} > 0 \\ &if\ h > h_c,\ \frac{dS^2}{d^2h} < 0 \end{aligned} \tag{2}$$

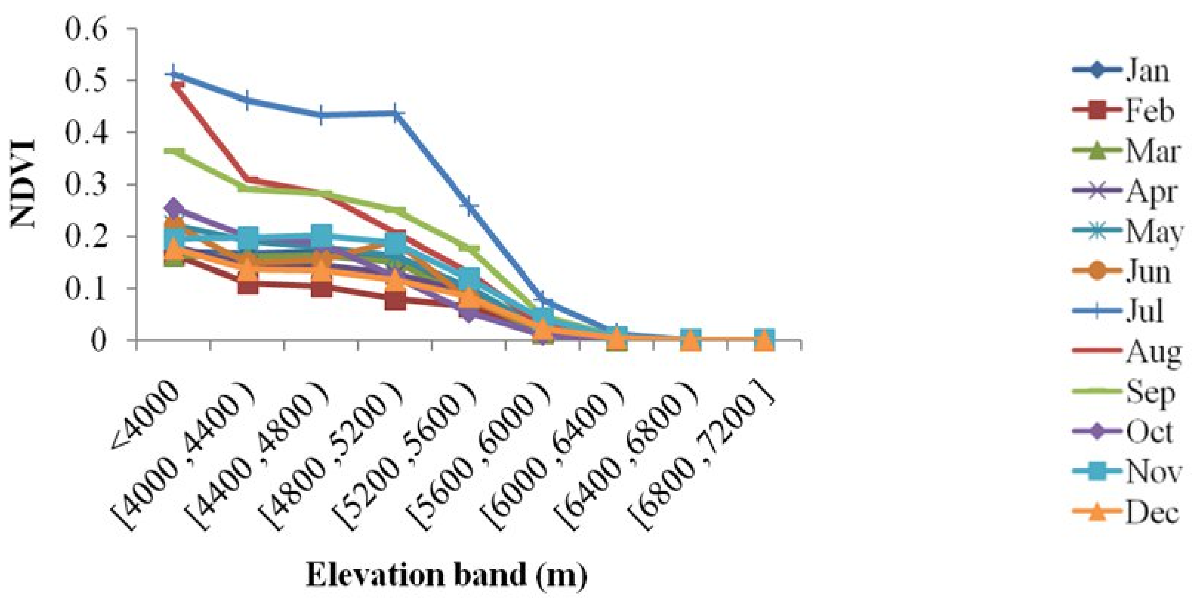

Figure 10. Relation between monthly NDVI and elevation from 2003 to 2005 with an elevation interval of 400 m

The relation of NDVI-Month at different elevation zones (Fig. 5) is converted to the relation of NDVI-Elevation in different months (Fig. 10). A pair of similar but reversed graphs of SCA-Elevation and NDVI-Elevation is preliminarily derived.

5. Correlation between SCA-elevation and NDVI-elevation

In this section, a finer interval of 200 m is adopted for elevation division in order to provide an insight into the relation among SCA-NDVI-Elevation. SCA-Elevation and NDVI-Elevation are obtained during the same time period of 2003-2005. For each elevation band, the expected values of snow-cover percentage (E(S)) and NDVI (E(ndvi)) and standard deviation of snow-cover percentage (σ(S)) and NDVI (σ(ndvi)) are derived from 12-month data. The values of E(S)±σ(S) and E(ndvi)±σ(ndvi) are used to represent the variability of SCA and NDVI within a year for every elevation band.

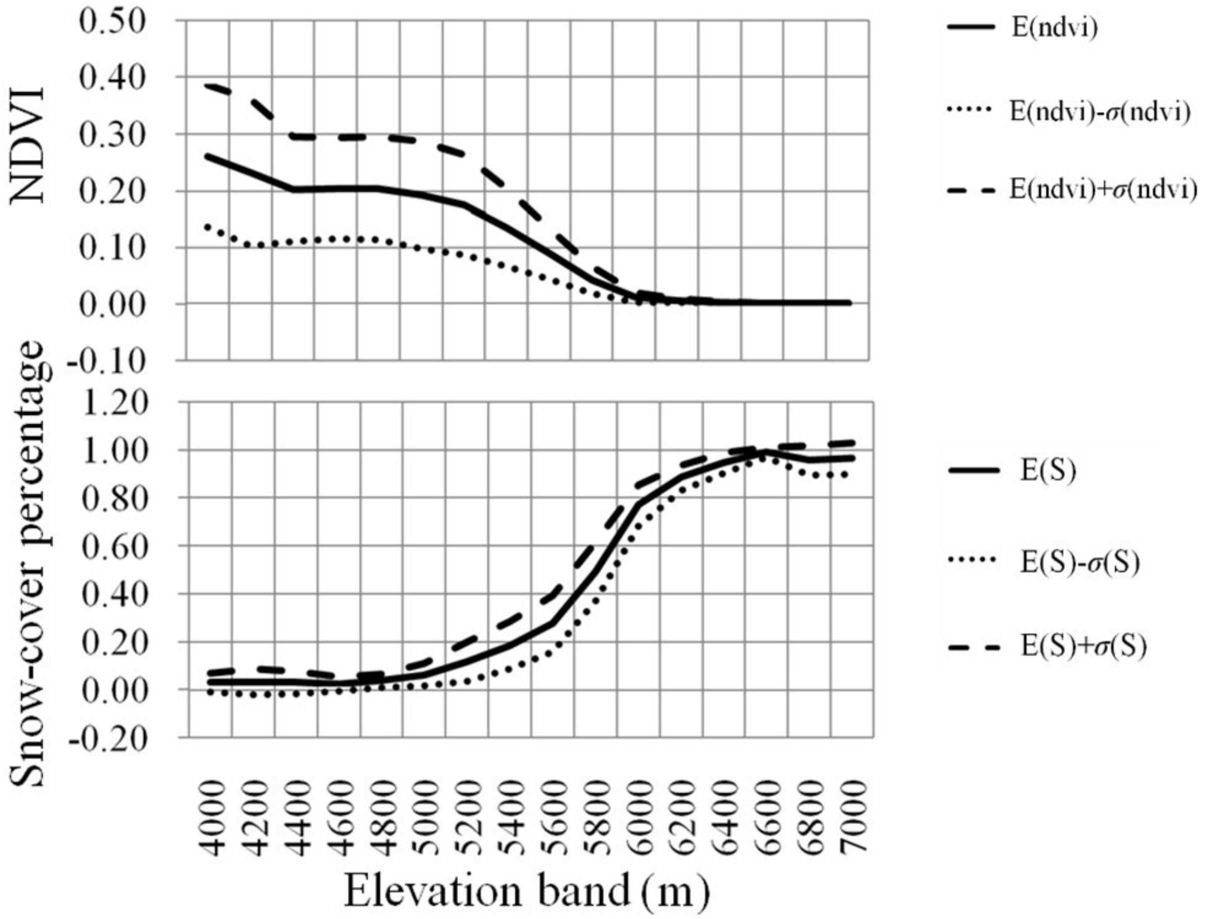

Figure 11. Relation among Snow-covered percentage, NDVI and elevation with an elevation interval of 200 m (h =200m). They look like each other, but reversed.

From Fig. 11, SCA increases, while vegetation cover decreases as elevation rises. Although a linear relationship between temperature and elevation is commonly used as "lapse rate", and both snow and vegetation are closely related to temperature, neither Snow-Elevation nor Vegetation-Elevation seems to be linear, as shown in Fig. 11. Furthermore, as elevation increases, both snow and vegetation follow the changing style of being gradually varying, rapidly varying and gradual varying again.

For variance:

Vegetation takes on a significant seasonality at low elevation, which leads to a high variance ($max\{\sigma(\text{ndvi})\}$= 0.13, at the elevation band of [4000,4200] meters above sea level (m.a.s.l)) at low elevation sites. As elevation increases, the seasonal variability decreases (shown in Fig. 12). In the SCA-Elevation curve, a high variability with maximum of σ(S) (= 0.12) occurs at the elevation band of [5600, 5800] m.a.s.l, where air temperature keeps above 0°C only in summer months (June, July, August) (shown in Table 1) (shown in Fig. 13). It suggests that there is sufficient snow because it is always cold enough to maintain snow in winter season, while hot enough to melt snow during summer season. Those contribute to high variability in snow regime. It also indicates that during summer season snowmelt strongly influence underlaying surface and snow regime in this region, which result in an intensive interaction between snow and vegetation in this region, such as the interception of vegetation could reduce snow accumulation and prolonged snow-covered periods would shorten vegetative growing season.

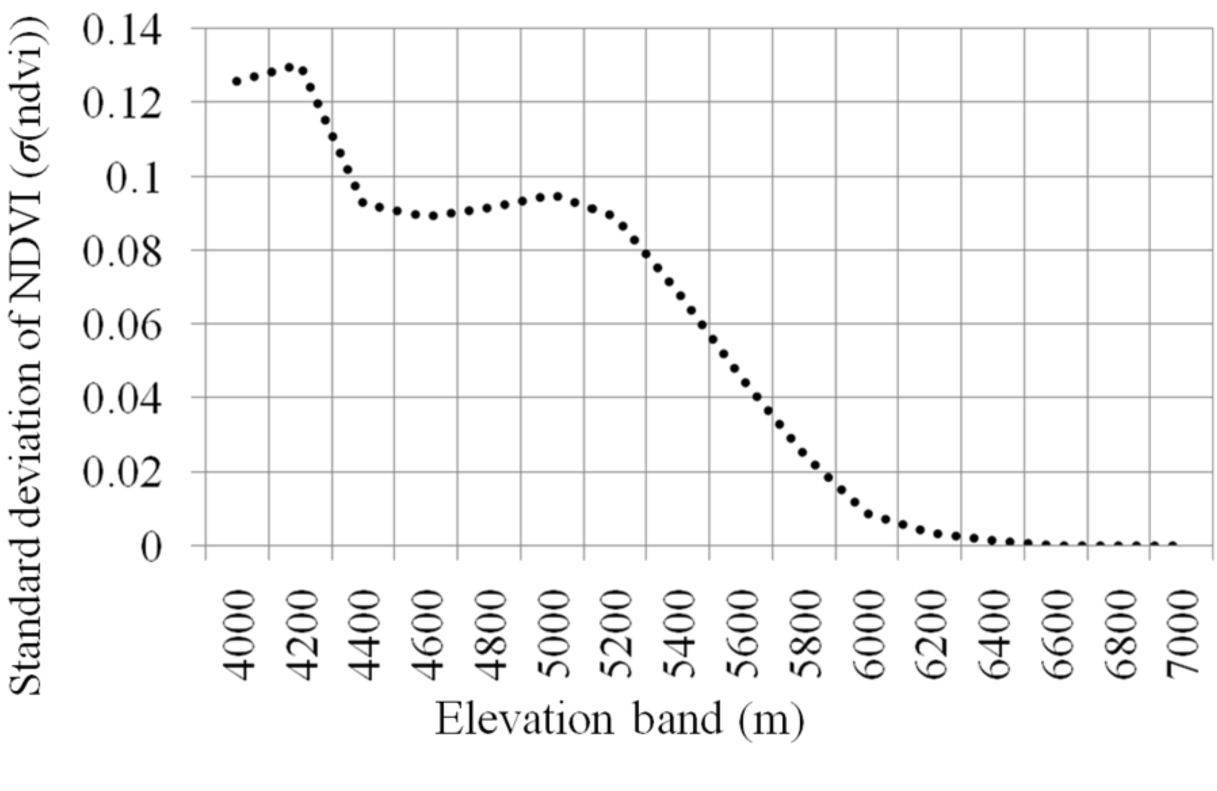

Figure 12. Variability of NDVI in a year. Variability increases as elevation decreases, which indicates an obvious seasonality for vegetation at low elevation sites, where vegetation grows well. As elevation increases, the seasonality diminishes.

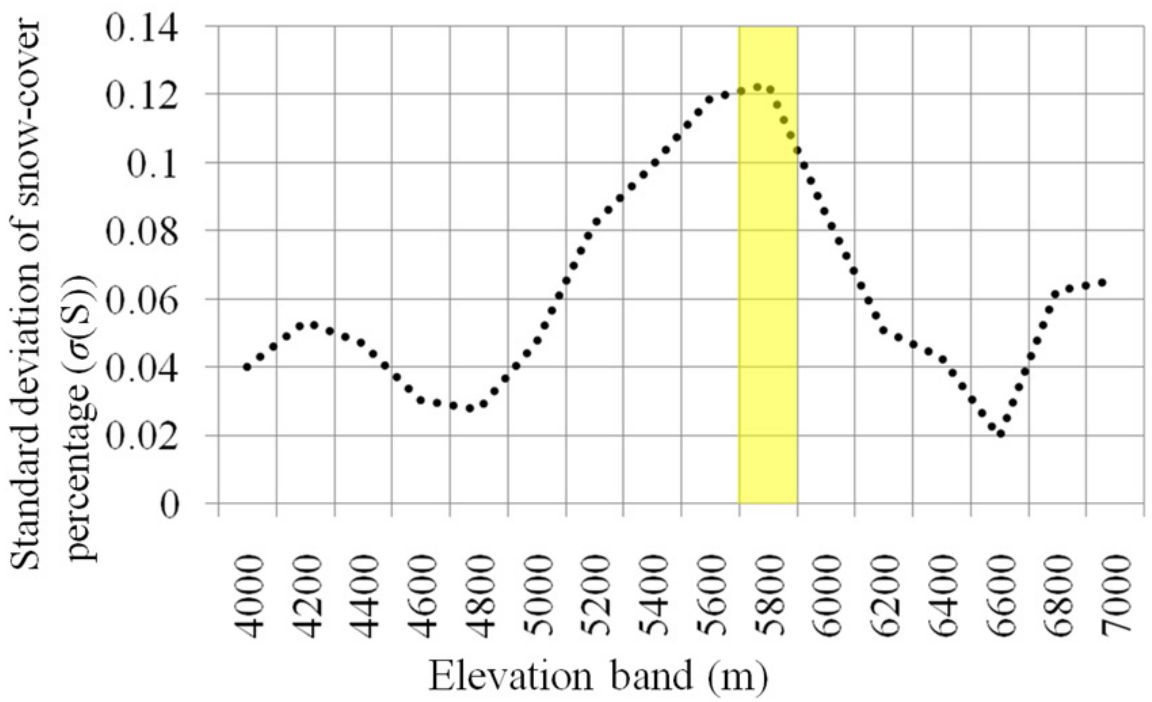

Figure 13. Variability of snow-cover percentage in a year

For expected value:

Knowledge in second derivative could offer a quantitative analysis. Second derivative illustrates how the rate of change proceeds for a given system. It could also be reflected by the curvature or concavity of a graph. A positive second derivative is illustrated by an upward curve (concave up), whereas a negative second derivative is denoted by a downward curve (concave down). The point switch from concave up to concave down is an inflection point. Based on the definition of the second derivative,

$$f''(S) = \lim_{h \to 0} \frac{\frac{f(S+h)-f(S)}{h} - \frac{f(S)-f(S-h)}{h}}{h} = \lim_{\Delta h \to 0} \frac{f(S+h)-2f(S)+f(S-h)}{h^2} \quad (3)$$

Here, $f(S+h)$ represents the snow-cover percentage / NDVI at upper elevation band, $f(S)$ is the snow-cover percentage / NDVI at middle elevation band, and $f(S-h)$ denotes the snow-cover percentage / NDVI at lower band.

The expression on the right only involves two variables: S (snow-cover percentage / NDVI) and h (elevation interval). As elevation interval is set to 200 m, we adopt the equation $f(S+h)-2f(S)+f(S-h)$ to calculate the second derivative.

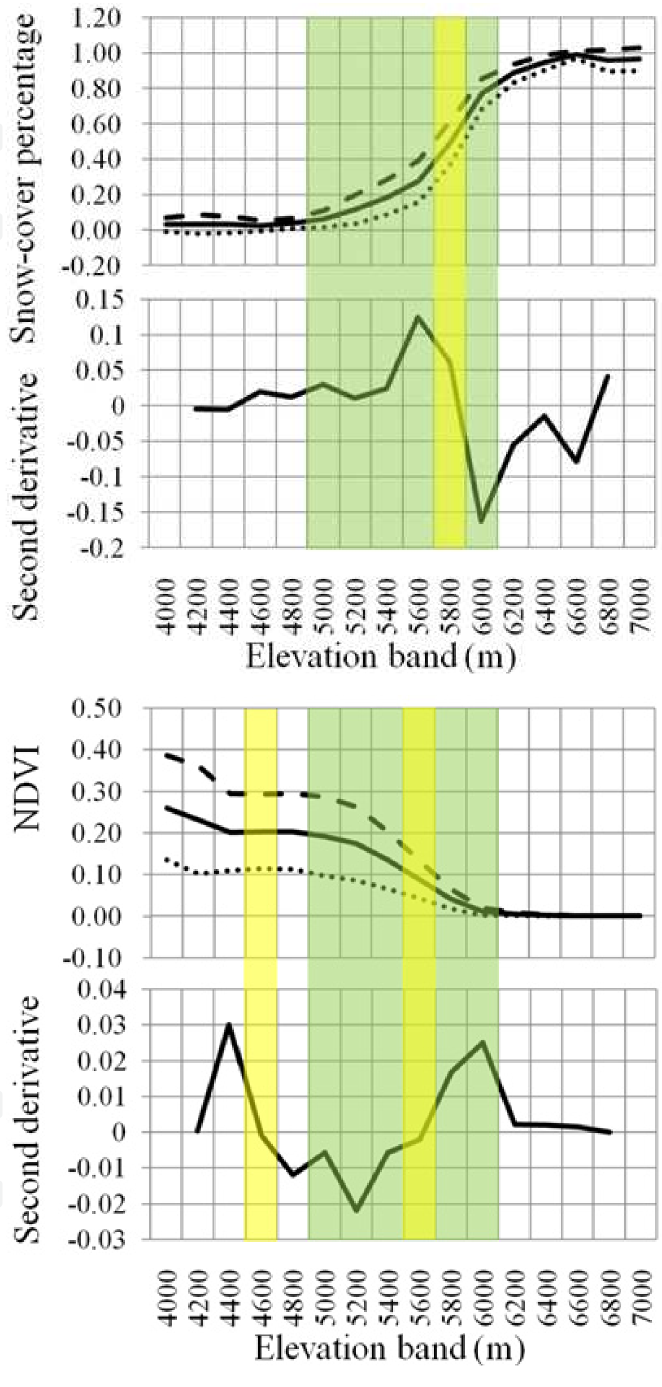

Figure 14. Second derivatives of SCA-elevation curve and NDVI-elevation curve

The second derivative demonstrates one inflection point in SCA-Elevation curve and two inflection points in NDVI-Elevation curve. As shown in Fig. 14, SCA-Elevation curve varies from concave up to concave down, with inflection point in the band of [5600, 5800] m.a.s.l. It suggests an accelerated growth below 5600 m and decelerated growth above 5800 m. Two inflection points in the band of [4400, 4600] and [5400, 5600] m.a.s.l divide NDVI-Elevation curve into three segments, from concave up to concave down then to concave up again:

1. ≤4400 m, vegetation decelerated decreases as elevation increase;
2. In the bands of [4600, 5400] m.a.s.l, vegetation acceleration decreases as elevation increase;
3. ≥5600 m, vegetation decelerated decreases as elevation increase.

According to Section 3, less than 20% of the area below 4800 m is seasonally covered by snow, where air temperature keeps above 0°C for more than 6 months (see Table 1). In the regions above 6000m, NDVI value is less than 0.01 and air temperature remains below 0°C during the whole year (see Table 1). Therefore, the coincident regions [4800, 6000] m.a.s.l for both snow and vegetation are meaningful and highlighted (Fig. 14).

Within the bands of [4800, 6000] m.a.s.l, the negative NDVI-Elevation curve varies from concave down to concave up with an inflection point in the band of [5400, 5600] m.a.s.l. On the other hand, the positive SCA-Elevation curve changes from concave up to concave down with an inflection point in the band of [5600, 5800] m.a.s.l. A nearly completed reversed relation between NDVI-elevation and snow-elevation is obtained.

6. Conclusion

Based on the Snow-Vegetation-Elevation relation derived from MODIS snow and MODIS vegetation products with a spatial resolution of 500 m, we discovered the following:

1. A positive relation between snow and elevation exists because temperature decreases as elevation increases. However, the quantification of SCA-Elevation relation derived in Yangbajain Basin, a branch of Lhasa River Basin, Tibet, China, demonstrates an "S"-shaped curve. This means that the SCA-Elevation does not follow the supposed linear shape of temperature lapse rate to elevation.
2. Phenological traits of vegetation are closely related to temperature, followed by elevation. However, a complex nonlinear relation between NDVI (an index of vegetation greenness) and elevation is also discovered.

Combined with the analysis on temporal distribution of snow and vegetation in Section 3, the elevation zone of [4800, 6000] m.a.s.l seems sensitive to both snow and vegetation in our study area. Furthermore, within this elevation zone, both SCA-Elevation and NDVI-Elevation present an "S" shape, initially having an accelerated variation followed by a decelerated one, but in reversed directions. The inflection point of Vegetation-Elevation is located between 5400 and 5600 m, and that of Snow-Elevation is between 5600 and 5800 m. It reveals that the NDVI-Elevation relation could be an indication of Snow-Elevation relation. In fact, there is really a very close interaction between snow and vegetation, such as interception of vegetation could reduce snow accumulation and long snow-covered periods would shorten vegetative growing season (Palacios, 1997; Buus-Hinkler et al., 2006). That is why the inflection of NDVI-Elevation almost coincide with inflection of Snow-Elevation relation, which could help to develop the linear Snow-Temperature-Elevation relation into a more complex function for a better model input.

1. It is also consistent with the point that the forest cover is the most highly correlated variable with snow cover (Varhola, 2010) at meso-scales (100–10 km), but mainly in snow-vegetation sensitive elevation. At relatively high elevations such as from 801 to 1069m accounting for a maximum about 1000m and >851/1200 in southeast British Columbia (D' Eon, 2004), or >6000 m/6970 m for Yangbajain Basin, greater snow versus reduced vegetation make the NDVI-Snow indication meaningless.
2. This book chapter provides a quantitative method to detect the Snow-NDVI-Elevation relation. It is a simple method that could be adopted in other watersheds for more comparisons and new findings.

Author details

Gao Jie
Hydrochina Corporation,
Beijing,
China

7. References

Anderton, S. P., White, S. M., & Alvera, B. (2002). Micro-scale spatial variability and the timing of snow melt runoff in a high mountain catchment. *Journal of Hydrology*, 268: 158-176.

Barry, R. G. (1992). *Mountain Weather and Climate*, *2nd edn*. Routledge, London: 402.

Bell, V. A., & Moore, R. J. (1999) .An elevation-dependent snowmelt model for upland Britain. *Hydrological Processes*, 13: 1887-1903.

Buus-Hinkler, J., Hansen, B. U., Tamstorf, M. P., & Pedersen, S. B. (2006). Snow-vegetation relations in a high arctic ecosystem: inter-annual variability inferred from new monitoring and modeling concepts. *Remote Sens. Environ*. 105, 237-247.

D' Eon, R. (2004). Snow depth as a function of canopy cover and other site attributes in a forested ungulate winter range in southeast British Columbia. *BC J. Ecosyst. Manage*. 3, 1-9.

Daugharty, D., & Dickinson, B. (1982). Snow distribution in forested and deforested landscapes in New Brunswick, Canada. *Proceedings of the 39th Eastern Snow Conference, Reno*, NV, April 19-23, 1982:10-19.

Essery, R.L., Pomeroy, J.W., Parvianen, J., & Storck, P. (2003). Sublimation of snow from coniferous forests in a climate model. *J. Climate*. 16, 1855-1864.

Gao, J., Wang, G. Q., Fu, X. D., Wang, H., & Gong, T. L. (2010). A research on spatial and temporal distribution of snow cover in Yangbajain Basin of Lhasa River Basin based on MODIS snow product. *Proceedings of The international conference on multimedia technology——Special Workshop on Geoscience and Remote Sensing*, Ningbo, China:1131-1137.

Gao, J., Williams, W. M., Fu, X. D., Wang, G. Q., & Gong, T. L. (2012). Spatiotemporal distribution of snow in Eastern Tibet and the response to climate change. *Remote Sensing of Environment*, doi:10.1016/j.rse.2012.01.006.

Han, Q. H., Wang, P. C., Wang, Y. K., Wang, J. K., Chen, W. M. & Gao, J. (2007). Characters of winter snow-cover and climate in Northeast China revealed by MODIS products, *Journal of Nanjing Institute of Meteorology*. 30, 3: 396-401. (In Chinese)

Hantel, M., Ehrendorfer, M., & Haslinger, A. (2000). Climate sensitivity of snow cover duration in Austria. *International Journal of Climatology*, 20(6): 615-640.

Hedstrom, N.R., & Pomeroy, J.W. (1998). Measurements and modeling of snow interception in the boreal forest, *Hydrol. Proc*. 12, 1611-1625.

Hendrick, R.L., Filgate, B.D., & Adams, W.M. (1971). Application of environment analysis to watershed snowmelt. *J. Appl. Meteorol*. 10, 418-429.

Hope, A.S., Boynton, W.L., Stow, D.A., & Douglas, D.C. (2003). Interannual growth dynamics of vegetation in the Kuparuk River watershed, Alaska based on the Normalized Difference Vegetation Index. *Int. J. Remote Sens*. 24, 3413-3425.

Hope, A.S., Pence, K.R., & Stow, D.A. (2004). NDVI from low attitude aircraft and composited NOAA AVHRR data for scaling Arctic ecosystem flux. *Int. J. Remote Sens*. 25, 4237-4250.

Huang, X. D., Zhang, X. D., Li, X. & Liang, T, G. (2007). Accuracy Analysis for MODIS Snow Products of MOD10A1 and MOD10A2 in Northern Xinjiang Area, *Journal of Glaciology and Geocryology*. 29, 5: 722-729. (In Chinese)

Jia, G. J., Epstein, H. E., & Walker, D. A. (2004). Controls over intra-seasonal dynamics of AVHRR NDVI for the Arctic tundra in northern Alaska. *Int. J. Remote Sens*. 25, 1547-1564.

Jost, G., Weiler, M., Gluns, D.R., & Alila, Y. (2007). The influence of forest and topography on snow accumulation and melt at the watershed-scale. *J. Hydrol*. 347, 101-115.

Li, P. J. (1995). Distribution of snow cover over the high Asia. *Journal of Glaciology and Geocryology*, 17, 4: 292-295. (In Chinese)

Li, X. G., & Williams, M. W. (2008). Snowmelt runoff modelling in an arid mountain watershed, Tarim Basin, China. *Hydrological Processes*, 22(19): 3931-3940.

Liston, G.E. (2004). Representing subgrid snow cover heterogeneities in regional and global models. *J. Climate*. 17, 1381-1397.

Ma, H., & Cheng, G.D. (2003). A test of Snowmelt Runoff Model (SRM) for the Gongnaisi River basin in the western Tianshan Mountains, China. *Chin. Sci. Bull*. 48(20), 2253-2259.

Marchand, M.D., & Killingtveit, A. (2005). Statistical probability distribution of snow depth at the model sub-grid cell spatial scale. *Hydrol. Proc*,19, 355-369.

McKay, G.A., & Gray, D.M. (1981). *The distribution of snowcover. In: Handbook of Snow: Principles, Processes, Management and Use*, Gray D M, Male D H (eds). Pergamon Press: Toronto; 153-190.

Myneni, R.B., Keeling, C.D., Tucker, C.J., Asrar, G., & Nemani, R.R. (1997). Increased plant growth in the northern high latitudes from 1981 to 1991. *Nature*, 386, 698-702.

Palacios, D., & García Sánchez-Colomer, M. (1997). The distribution of high mountain vegetation in relation to snow cover: Penalara, Spain. *Catena*. 30, 1-40.

Williams, M.W., Rebecca, T., Barnes, R. T., Parman, J. N., Freppaz, M., & Hood, E. (2011). Stream Water Chemistry along an Elevational Gradient from the Continental Divide to the Foothills of the Rocky Mountains. *Vadose Zone Journal*, doi:10.2136/vzj2010.0131, 10:900-914

Pomeroy, J., Gray, D., Hedstrom, N., & Janowicz, J. (2002). Precipitation of seasonal snow accumulation in cold climate forests, *Hydrol. Proc*. 16, 3543-3558.

Qin, D. H., Xiao, C. D., Ding, Y. J., Yao, T. D., Bian, L. G., Ren, J. W., Wang, N. L., Liu, S. Y. & Zhao, L. (2006). Progress on cryospheric studies by international and Chinese communities and perspectives, *Journal of Applied Meteorological Science*. 17, 6: 649-656. (In Chinese)

Sloan, W. T., Kilsby, C. G., & Lunn, R. (2004). Incorporating topographic variability into a simple regional snowmelt model. *Hydrological Processes*, 18: 3371-3390.

Varhola, A., Coops, N.C., Weiler, M., & Moore, R.D. (2010). Forest canopy effects on snow accumulation and ablation: An integrative review of empirical results. *J. Hydrol*. 392, 219-233.

Wen, J., Dai, M., Deroin, J. P., Wang, Z. J., & Humber, L. (2006). Extent and depth of snow cover over the Nyaingentanghla Range derived from ASAR and MODIS data, *Journal of Glaciology and Geocryology*. 28, 1: 54-61. (In Chinese)

Winkler, R. D., Spittlehouse, D. L., & Golding, D. L. (2005). Measured differences in snow accumulation and melt among clearcut, juvenile, and mature forest in southern British Columbia. *Hydrol. Proc*. 19, 51-62.

Yang, Z. N., Liu, X. R. & Zeng, Q. Z. (2000). *Hydrology in Chinese cold region*. Beijing: science press. (In Chinese)

Zhang, J., Han, T. & Wang, J. (2005). Changes of snow-cover area and snowline altitude in the Qilian Mountains, 1997-2004, *Journal of Glaciology and Geocryology*. 27, 5: 649-654. (In Chinese)